Desalination and Water Treatment
www.deswater.com

doi: 10.5004/dwt.2020.25854

195 (2020) 256–266
August

Study of the effects of ferric iron/ferrous iron ratio in influent AMD and hydraulic retention time on alkalinity generation, iron, aluminum and manganese removals by SAPS

M.D. Patel

Department of Mining Engineering, National Institute of Technology, Raipur, India, email: mdpatel.min@nitrr.ac.in

Received 6 July 2019; Accepted 18 March 2020

ABSTRACT

Acid mine drainage (AMD) is a major worldwide environmental threat since it is the source of water deterioration with harmful effects on aquatic life. Therefore, a cost-effective and efficient AMD treatment system needs to have experimented with a variety of AMD solutions. This research sought to investigate the effects of ferric iron/ferrous iron ratio, of influent AMD and hydraulic retention time (HRT) on alkalinity generation by laboratory successive alkalinity producing system (SAPS). The present study reveals that the alkalinity generation increases with an increase of ferric/ferrous iron ratio along with total iron and HRT with constant aluminum and manganese concentration. The maximum alkalinity generation achieved by SAPS treatment was 1,030; 1,210; 1,375; and 1,510 mg/L (in terms of $CaCO_3$ equivalence) for AMD A, AMD B, AMD C, and AMD D for 10 d HRT, respectively. The removal behavior of iron, aluminum, and manganese was also studied with four different AMDs. The maximum of 100% iron and aluminum removal and 42.67% of manganese removal was reported for AMD A for 10 ds HRT. Therefore, SAPS is found suitable and effective for the removal of iron and aluminum but in the case of manganese removal it is partially effective. The gradual sulfate reductions were also observed which confirm the microbial activity and metal removal. The above approach has a potential application for effective AMD treatment in mining fields.

Keywords: Successive alkalinity producing system; Hydraulic retention time; Acid mine drainage; ORP; DO

1. Introduction

One of the most challenging problems affecting the mine environment around the world is the efficient and effective treatment of acid mine drainage (AMD). The problem of AMD pollution is commonly observed in the mines of Australia, Canada, USA, India, and many other countries around the globe. The AMD adversely affects the surrounding aquatic environment by killing fish and other forms of aquatic biota. Besides this, it increases the corrosion in mining machinery and pipes and changes the soil chemistry on which AMD is discharged and consequently reduces the crop productivity. The USA Environmental Protection Agency (US-EPA) suggested that AMD be "Second only to global warming and ozone depletion" in terms of ecological risk [1]. Mining of the coal and metals exposes the pyrite minerals to oxygen and water, which coupled with bacterial activity, leads the formation of AMD that are highly enriched with sulfate, aluminum, and heavy metals [2–4]. Coal mine drainages in the USA are largely contaminated with dissolved iron and manganese [5]. Following chemical reactions are taking place during the formation of AMD [6].

$$FeS_2 + 3.5\,O_2 + H_2O \xrightarrow{\text{Bacteria}} Fe^{2+} + 2\,SO_4^{2-} + 2H^+ \quad (1)$$

$$Fe^{2+} + 2.5\,H_2O + 0.25O_2 \xrightarrow{\text{Bacteria}} Fe(OH)_3 + 2H^+ \quad (2)$$

$$FeS_2 + 14Fe^{3+} + 8H_2O \xrightarrow{\text{Bacteria}} 15Fe^{2+} + 2SO_4 + 16\,H^+ \quad (3)$$

$$FeS_2 + 14\,Fe^{3+} + 8H_2O \rightarrow 15\,Fe^{2+} + 2SO_4 + 16\,H^+ \quad (4)$$

The presence of microbial population not only plays a key role in AMD generation, but it also increases the corrosion and bioleaching of metals [7]. The AMD is characterized by a high concentration of iron, manganese, aluminum, and other metal along with low pH and acidity [8,9]. In dealing with AMD, one should focus on the minimization of the generation of AMD. If not then, it must be collected and treated effectively [10]. In the active treatment methods mainly chemicals such as sodium hydroxide, ammonia, etc., are used to raise the pH of water [11]. Many passive systems have been designed for treating AMD by using naturally occurring biological and chemical processes without using hazardous chemicals to treat AMD [12]. Successive alkalinity producing system (SAPS) has advantages of anaerobic wetlands and the efficiency of anoxic limestone drains. [13].

The main objective of this study is to investigate the alkalinity generation potential with respect to ferric/ferrous ratio and study of removal pattern of iron, aluminum, and manganese. The performance of SAPS is highly affected by influent AMD quality; therefore, research was undertaken to assess the effects of ferric/ferrous iron ratio on alkalinity generation and metal removal behavior.

2. Materials and methods

2.1. Experimental setup

A standard SAPS setup is designed for required experiments. In this SAPS set-up, four PVC containers of 80 L capacity were filled with limestone, gravel, sawdust, and organic substrate as shown in Fig. 1. In the bottom SAPS cell, a perforated pipe is fitted, which is connected to a standpipe and flush pipe outside the SAPS cell. The standpipe discharges treated AMD into oxidation cell and flush pipe fitted with a flush valve to flush out the SAPS cell's clogging, time to time for proper maintaining the flow condition inside the SAPS cell. Experiments were conducted with four different synthetic AMDs in the SAPS column with identical conditions having a similar composition of limestone, the organic substrate (cow compost), and sawdust in the same time period. Therefore, the effects of the above geometric and environmental parameters will be equal in all the SAPS, hence the effects of the above parameters were considered as a uniform for all the four SAPS operating simultaneously. The above experiments were conducted from 18°C to 32°C. SAPS cells were allowed for a 15 d acclimation period for enough growth of bacteria. After the acclimation period AMD solutions were allowed to flow in SAPS cell with a controlled flow rate with different (1, 2, 4, 7, and 10 d) hydraulic retention time (HRT). The flow rates were controlled with the help of intravenous infusion (I-V) set. The composition of four different synthetic AMD is given in Table 1.

2.2. Composition of synthetic AMD

The composition of synthetic AMDs was selected on the basis of findings of previous works of various researchers in the field of AMD and samples collected from coal mines (Table 1). More than 160 worldwide AMD data

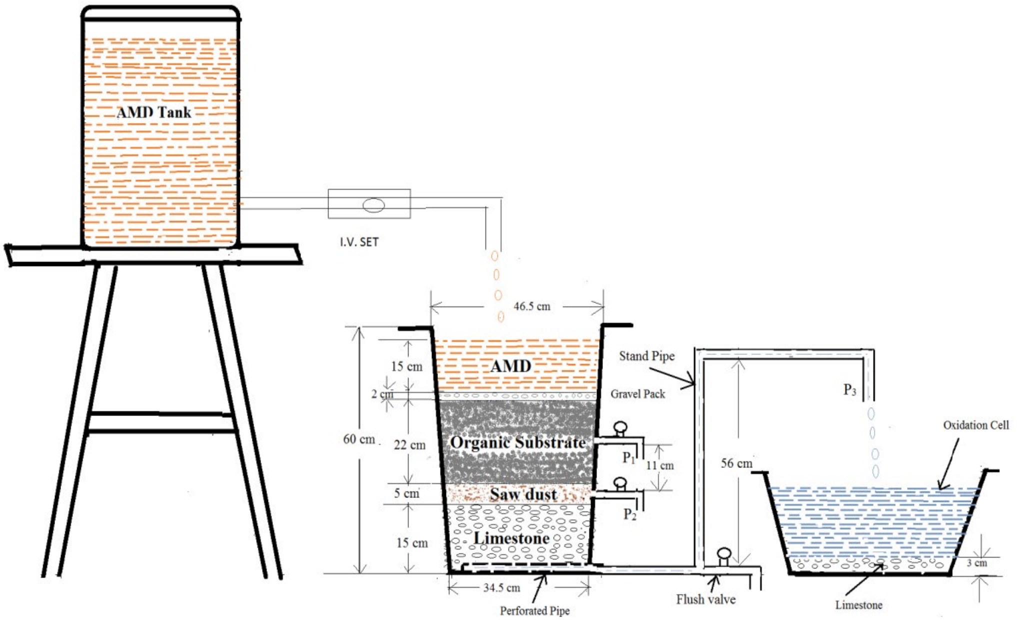

Fig. 1. Laboratory arrangement for SAPS column study [14].

were studied for the selection of synthetic AMD. A set of four AMDs was prepared having similar concentrations of aluminum (20 mg/L) and manganese (30 mg/L) with variations in iron and ferric/ferrous ratio.

2.3. Sampling and analysis

The AMD A, AMD B, AMD C, and AMD D were allowed to flow in SAPS A, SAPS B, SAPS C, and SAPS D respectively after 15 d acclimation period. Then all the samples were collected at port P_1, port P_2, and port P_3 for different HRT's of 1, 2, 4, 7, and 10 d, respectively.

The pH, DO, ORP, temperature and electrical conductivity of the collected sample are instantly measured by portable WTW multi 3620 IDS digital meter. Then alkalinity was determined by 0.02 N H_2SO_4 titration and acidity was also determined by 0.02 N NaOH titration on unfiltered samples. The collected samples were filtered in the Whatman membrane filter (0.45 μm) and acidified with HNO_3 and kept for further analysis in the refrigerator at 4°C. The determination of ferrous iron and total iron was carried out using 1, 10-phenanthroline solution and ammonium acetate buffer solution by spectrophotometer. The ferric iron was calculated as the difference between total iron and ferrous iron. Aluminum was determined using the Eriochrome cyanine R spectrophotometer method. Manganese was determined using ammonium persulfate by spectrophotometer. Sulfate determination was done by using the barium chloride method in the spectrophotometer. The Lasany UV-VIS spectrophotometer was used in the above-mentioned tests. Calcium and magnesium were determined by EDTA method. The flow rates were measured by volumetric cylindrical flask and stops watch. All the measurements was carried out as per standard methods of APHA unless specified [15].

3. Results and discussion

3.1. ORP and DO variations

The ORP in SAPS cell A for AMD A at port P_3 showed a downward trend from 106.30 to –211.40, –212.40, –311.30, –318.30, and –317.70 mV, which indicated that a strongly reducing environment was prevailing inside the SAPS cell A. The negative ORP inside the SAPS is an essential condition for the efficient operation of SAPS system. The DO levels in SAPS cell A for AMD A were dropped from 6.42 to 0.06, 0.00, and 0.00 mg/L for port P_1, port P_2, and port P_3, respectively for 1 d HRT. Similar trends were reported for 2, 4, 7, and 10 d HRTs. The DO level dropped to 0.00 mg/L at port P_3 for all HRTs, which is an encouraging indicator of the attainment of anaerobic conditions inside the SAPS cell. Therefore, DO and ORP changed status is favorable for the anaerobic reducing environment inside all the four SAPS cells. Similar trends we are reported for ORP and DO status for SAPS B, SAPS C, and SAPS D, with AMD B, AMD C, and AMD D loadings, respectively. The electrical conductivity and sulfate were decreasing during the SAPS process which confirmed the metal removals and alkalinity generation in SAPS cell. The alkalinity generation in the form of bicarbonate (HCO_3^-) can be represented by the following equation:

Table 1
Compositions of AMDs used in experiments

	AMD A	AMD B	AMD C	AMD D
pH	4.45	3.65	2.75	2.58
ORP (mV)	106.3	105.30	108.40	108.30
DO (mg/L)	6.42	7.12	6.48	5.82
Total Fe (mg/L)	91.70	129.70	174.00	194.35
Fe^{2+} (mg/L)	82.30	96.50	81.70	107.20
Fe^{3+} (mg/L)	9.40	33.20	92.30	87.15
(Fe^{3+}/Fe^{2+}) ratio	0.114	0.340	1.130	1.230
Al (mg/L)	20.00	20.00	20.00	20.00
Mn (mg/L)	30.00	30.00	30.00	30.00
Ca (mg/L)	125.00	125.00	125.00	125.00
Mg (mg/L)	100.00	100.00	100.00	100.00
SO_4^{2-} (mg/L)	1,031.00	1,037.00	1,041.00	1,036.00
Electrical conductivity μs/cm	1,950	1,996	2,152	2,171

$$2CH_2O + SO_4^{2-} \rightarrow H_2S + 2HCO_3^- \quad (5)$$

where CH_2O represents organic matter [13].

3.2. pH variations

All four SAPS showed remarkable continuous improvements in pH level during treatment. The maximum pH was raised to 8.55, 8.55, 8.40, and 8.35 for AMD A, AMD B, AMD C, and AMD D for 10 d HRT respectively as shown in Figs. 2–5.

3.3. Effect of ferric iron/ferrous iron ratio on alkalinity generation

The total iron does not give any idea about their corresponding ferric and ferrous iron concentrations. The ferric/ferrous ratio is found higher in AMD and became reduced after treatment. Therefore, in this study ferric iron/ferrous iron ratio is taken as an important parameter. In the study ferric/ferrous ratio is denoted as R and total iron as TI. The combined iron factor F is taken as:

$$F = R \times TI \quad (6)$$

This would give more appropriate knowledge about the effect of iron on alkalinity generation by SAPS by keeping the concentration of aluminum and manganese constant between 20 and 30 mg/L for all four AMDs. The iron factor F and corresponding alkalinity generation are shown in Table 2.

It is clear from the Table, that the alkalinity generation by SAPS increases with an increase in iron factor ($F = R \times TI$) for a particular HRT at a constant aluminum concentration at 20 mg/L and manganese concentration at 30 mg/L in influent AMD's.

The increase in alkalinity generation with respect to an increase in iron factor F, for the four AMDs, is shown in Table 2. The alkalinity generation increases due to an increase in iron factor F, from 10.45 to 239.05 for all HRTs.

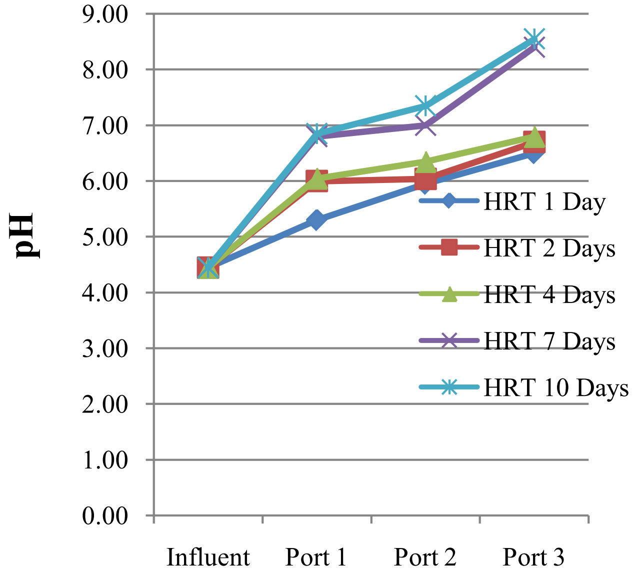

Fig. 2. pH variation in SAPS with AMD A.

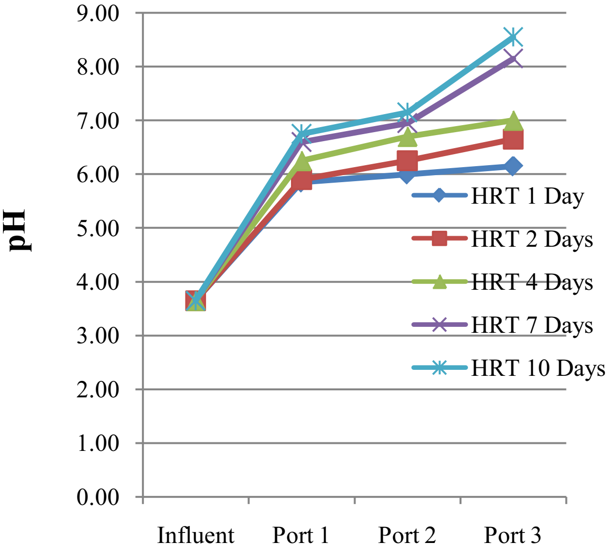

Fig. 3. pH variation in SAPS with AMD B.

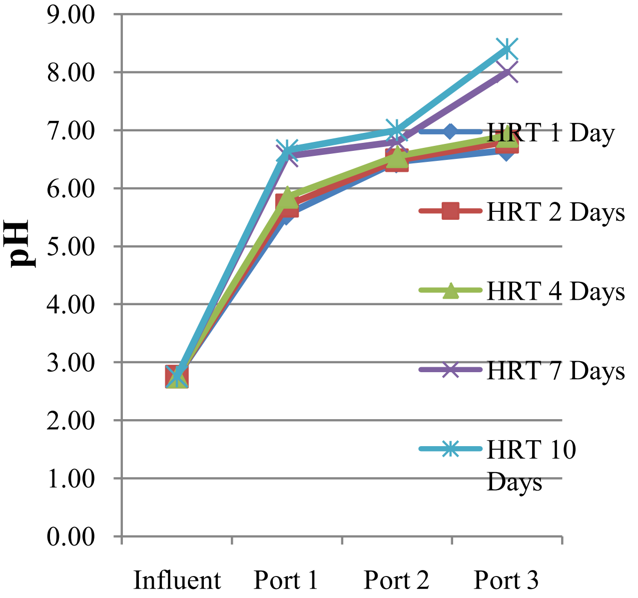

Fig. 4. pH variation in SAPS with AMD C.

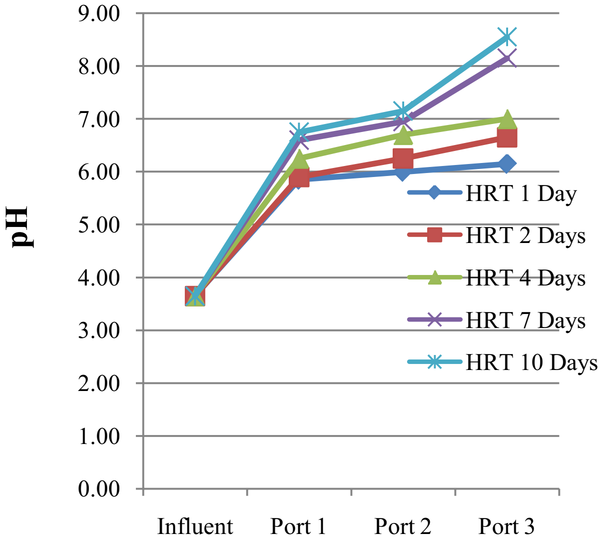

Fig. 5. pH variation in SAPS with AMD D.

Secondly, the increase in alkalinity generation is higher for longer HRT for a particular iron factor ($F = R \times TI$) at a constant aluminum concentration at 20 mg/L and manganese concentration at 30 mg/L in influent AMDs.

3.4. Effects of HRT on alkalinity generation

The effects of HRT on alkalinity generation are assessed at all three ports (P_1, P_2, and P_3). The alkalinity generation at port P_1 was reported as 150, 240, 280, 405, and 440 mg/L (all in terms of $CaCO_3$ equivalence) for 1, 2, 4, 7, and 10 d HRT's with a corresponding pH level of 5.30, 6.00, 6.05, 6.80 and 6.85, respectively as shown in Fig. 11. The continuous increases in alkalinity generation were observed for 1 d HRT to 10 d HRT at port P_1. Therefore, alkalinity generation is increasing with an increase in HRT duration because more time was available for microbial reactions and chemical reactions in the limestone layer.

The alkalinity generation further increases at port P_2. The observed alkalinity generation at port P_2 were 230, 385, 450, 565, and 625 mg/L (all in terms of $CaCO_3$ equivalence) for 1, 2, 4, 7, and 10 d HRTs with a corresponding pH level of 5.95, 6.04, 6.35, 7.00, and 7.35 respectively as shown in Fig. 6. In this zone alkalinity is generated by microbial activity in the organic substrate layer in the anaerobic environment inside the SAPS cell.

The generation of alkalinity increases at port P_3 because of the dissolution of limestone in the bottom layer. The alkalinity generation at port P_3 was reported as 435, 540, 700, 905, and 1,030 mg/L (all in terms of $CaCO_3$ equivalence)

Table 2
Iron factor *F* and corresponding alkalinity generation

AMD	Iron factor $F = R \times TI$	Alkalinity generation in mg/L as $CaCO_3$				
		HRT = 1 d	HRT = 2 d	HRT = 4 d	HRT = 7 d	HRT = 10 d
AMD A	10.45	435	540	700	905	1,030
AMD B	44.09	465	615	795	1,070	1,210
AMD C	196.62	660	815	1,000	1,250	1,375
AMD D	239.05	715	925	1,150	1,400	1,510

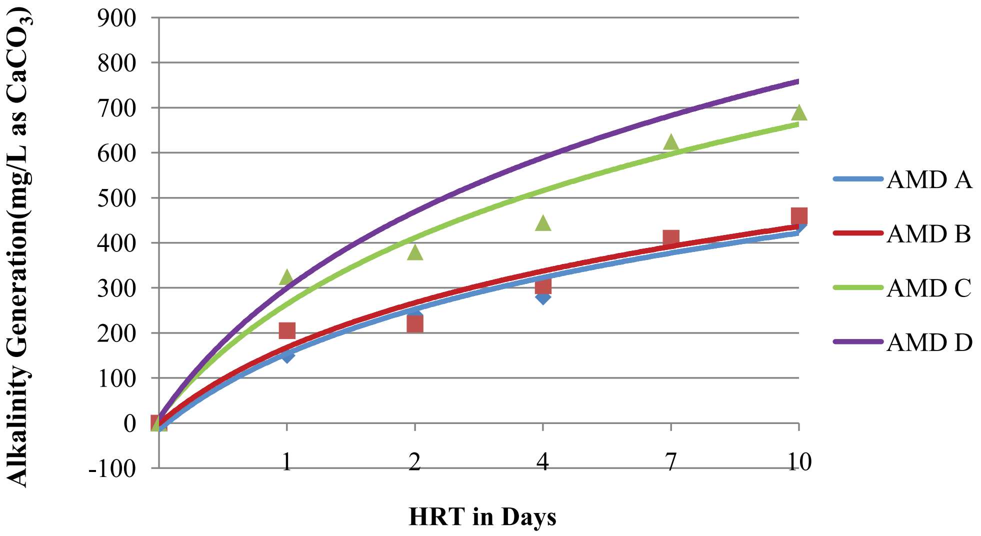

Fig. 6. Alkalinity generation in different HRT for port P_1.

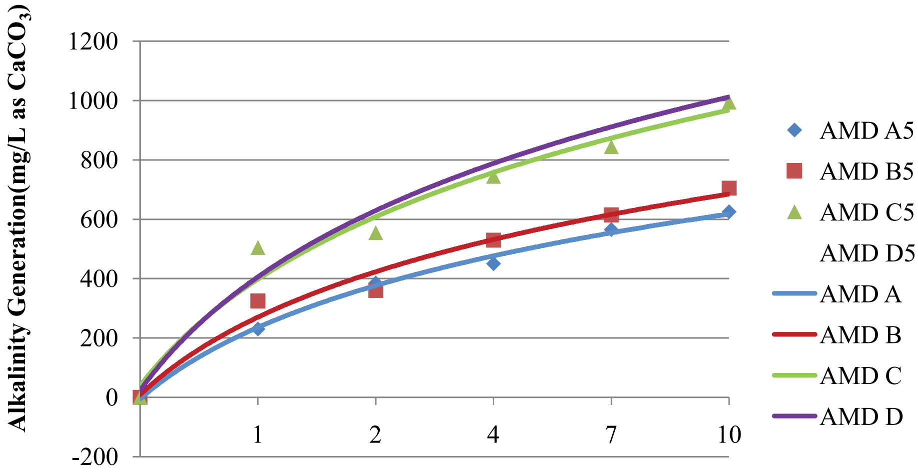

Fig. 7. Alkalinity generation in different HRT for port P_2.

for 1, 2, 4, 7, and 10 d HRT's with a corresponding pH level of 6.50, 6.70, 6.80, 8.40, and 8.55, respectively as shown in Fig. 8. The similar increasing trends of alkalinity generation were obtained for AMD B, AMD C, and AMD D as shown in Figs. 6–8.

Based on the above plots from Figs. 6–8 it is observed that the alkalinity generation by SAPS increases in a logarithmic manner with an increase in HRT in all three ports. The pH values in the four influent synthetic AMD's ranged from 2.58 to 4.45 and they were found to rise to a range from 8.35 to 8.55 at the discharge for 10 d HRT. The pH levels increased in all the four AMDs which confirmed the alkalinity generation by SAPS units. A strong reducing environment is observed inside the SAPS in organic substrate

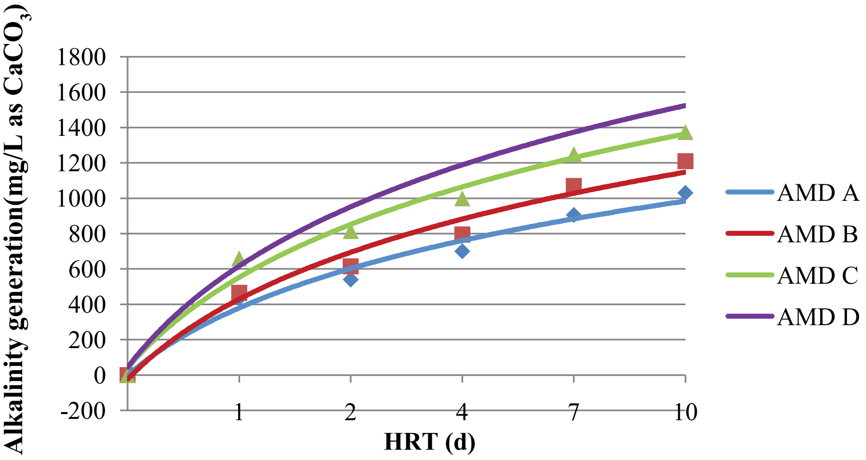

Fig. 8. Alkalinity generation in different HRT for port P_3.

thereby resulting in the precipitation of metal sulfide and bicarbonate alkalinity was generated simultaneously [16].

3.5. Iron removal behavior

It was observed that in AMD A, the iron removal percentage at port P_1 for HRT 1, 2, 4, 7, and 10 d were 0.11%, 0.11%, 3.82%, 59.00%, and 63.36%, respectively and pH was found increased from 4.45 to 5.30, 6.00, 6.05, 6.80, and 6.85 respectively as shown in Fig. 9. Further ferric iron was getting converted to ferrous iron in organic substrate layer in reducing environment therefore ferric iron concentration was reduced from 9.40 to 1.60, 1.40, 1.20, 0.00 and 0.00 mg/L at port P_1 for 1, 2, 4, 7, and 10 d HRTs, respectively. Hence same can be justified with an increase in ferrous iron concentration from 82.30 to 90.00, 90.20, and 87.00 mg/L at port P_1 for 1, 2, and 4 d HRTs, respectively up to pH level 6.05.

The observed cumulative iron removal percentage at port P_2 for HRT of 1, 2, 4, 7 and 10 d were 0.22%, 2.62%, 24.10%, 70.23%, and 88.11% respectively and pH increased to 5.95, 6.04, 6.35, 7.00, and 7.35, respectively as shown in Fig. 10. Significant removal of iron at port P_2 took place from 2 d HRT and onwards. Similarly, complete reduction of ferric iron at port P_2 was observed except for two HRTs (i.e., 1.30 and 1.10 mg/L for 1 and 2 d). Therefore, it is clear that all the ferric iron was reduced to ferrous iron in the organic substrate layer.

A continuous increasing trend in iron removal with increasing HRTs was observed at port P_3. The observed cumulative removal percentage at port P_3 for 1, 2, 4, 7, and 10 d HRT were 15.05%, 36.10%, 59.00%, 100%, and 100%, respectively with corresponding pH increase to 6.50, 6.70, 6.80, 8.40, and 8.55, respectively as shown in Fig. 11. Port P_3 is the most important terminal because it discharges the treated AMD in the oxidation cell and again oxic condition prevails therefore we can assess the performance of SAPS cells by analyzing the discharged treated AMD from port P_3. It has been observed that iron present at this stage is found in ferrous form. In port P_3, 100% iron removal was observed for 7 and 10 d HRTs whereas less removal percentage was reported for 1, 2, and 4 d HRTs therefore iron removal increases with an increase in HRT.

A similar increasing trend in iron removal like AMD A was observed with AMD B, AMD C, AMD D. The significant iron removal at port P_1 for all AMD B, AMD C, and AMD D was initiated after 4 d HRT and complete removal were achieved at port P_3 after 7 d HRT for all the three AMDs as shown in Figs. 9–11. The complete iron removal was observed at port P_3 in most of the cases for 7 d HRT. The iron removal percentage at port P_3 for 4 d HRT ranges from 59.00% to 70.16%. Similar significant iron removal of 87.7% with SRB bioreactor was reported in the study by Choudhary and Sheoran [17] and Genty et al. [18], wherein it was observed that at shorter HRT the growth of SRB was not sufficient for precipitation of iron.

3.6. Aluminum removal behavior

In influent AMD A the aluminum concentration was 20.00 mg/L which dropped subsequently during the treatment process by SAPS. The aluminum removal at port P_1 was reported as 65.00%, 75.00%, 85.00%, 100%, and 100% respectively for 1, 2, 4, 7, and 10 d HRTs duration which the corresponding level of 5.30, 6.00, 6.05, 6.80, and 6.85 respectively as shown in Fig. 12 where the initial pH level of influent AMD A was 4.45. The increasing trends in pH levels were observed during the treatment process with respect to the duration of HRTs. Aluminum started to precipitate as $Al(OH)_3$ from a pH level of 5.30 an onwards in the SAPS system. The above results are as per the expectation of aluminum chemistry.

In port P_2 further increase in aluminum removal was observed. The aluminum removal at port P_2 was 75%, 100%, 100%, 100%, and 100% for 1, 2, 4, 7, and 10 d HRTs duration which the corresponding level of 5.95, 6.04, 6.35, 7.00, and 7.35, respectively as shown in Fig. 13.

All aluminum contamination was removed at port P_3 for each HRT duration as shown in Fig. 14. Aluminum is the first metal to precipitate a SAPS cell. Aluminum precipitation takes place inside the SAPS and deposited in void space available inside the organic substrate. That is why the time to

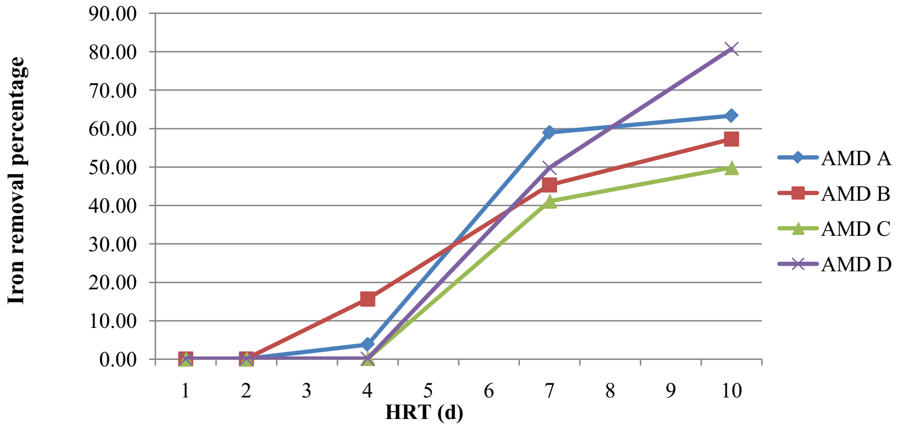

Fig. 9. Iron removal percentage in port P_1.

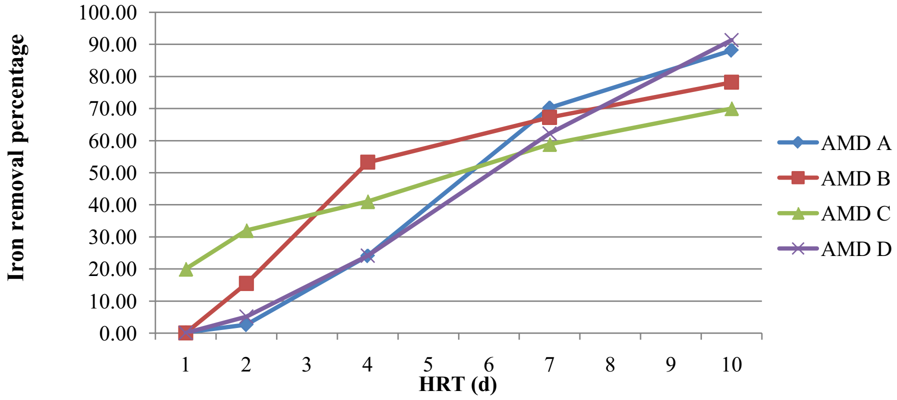

Fig. 10. Iron removal percentage in port P_2.

time flushing of SAPS cells is required to avoid clogging of pore space of organic substrate and limestone layer.

The similar increasing trends like AMD A were also observed for all three AMDs, that is, AMD B, AMD C, and AMD D as shown in Figs. 12–14. The precipitation of Al took place from pH level of 5.05 and onwards for AMD D. The complete removals of Al took place after 7 d HRT for all the three AMDs when the pH level was around 7.00. The SAPS showed efficient performances for aluminum removal in all the experiments, where 100% removal was achieved. Aluminum has a higher precipitation tendency as compared to iron to form hydroxide at a pH level of 5–6 [19].

3.7. Manganese removal behavior

The manganese concentration in influent AMD A was 30 mg/L. At port P_1 for different HRT's Mn has been reduced from 0.40 to 0.50 mg/L. The reason for the above reduction is the adsorption of manganese by the organic substrate. Further no significant Mn removals were reported at port P_1 for all 1, 2, 4, 7, and 10 d HRTs duration as shown in Fig. 15.

Similar observations as port P_1 have been observed at port P_2 for all 1, 2, 4, 7, and 10 d HRTs duration as shown in Fig. 16.

No significant manganese removals were observed port P_3 for 1, 2, and 4 d HRTs but 28.33% and 42.67%. Mn removal was observed for 7 and 10 d HRTs respectively with corresponding pH level 8.40 and 8.55 respectively as shown in Fig. 17.

Similar trends in Mn removal were observed for all three AMDs, that is, AMD B, AMD C, and AMD D. The Mn removal was started when the pH level reached near 8.00 as shown in Figs. 15–17. It was overall observed that at port P_3, that is, effluent end of SAPS unit, the significant manganese removal was observed after raising the pH of AMD solution to 8 and above for 7 d and 10 d HRTs. The maximum manganese removal was reported as 42.67% for AMD A and AMD B in experiments for 10 d HRT at a pH level of 8.55. In this research work, complete removal of manganese was not attained in the SAPS system. The similar partial 28% manganese removal inside the SAPS for 3.5 d HRT was also reported by Ordonez et al. [20].

The pH level of more than 8 is essential for oxidizing manganese(II) to insoluble manganese(IV). The manganese removal started significantly only after the removal of iron. Similar findings were also observed by Hallberg and Johnson [21]. The observations of experiments are in agreement with the statement that the presence of Fe(II) inhibits manganese precipitations as given by Sapsford and

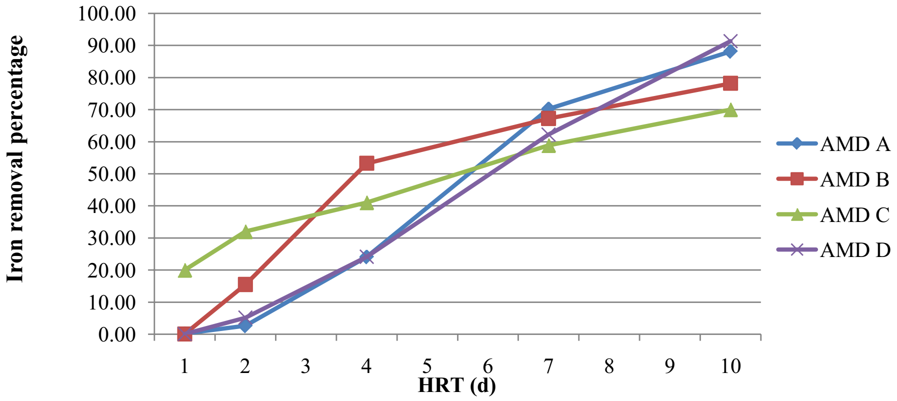

Fig. 11. Iron removal percentage in port P_3.

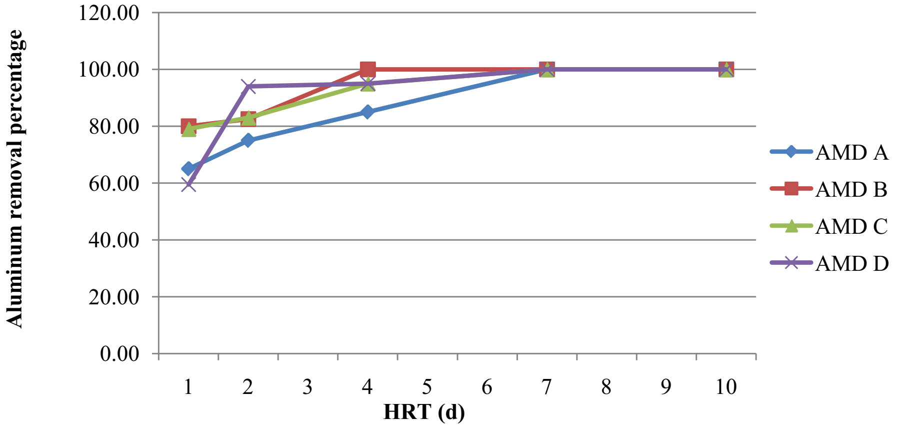

Fig. 12. Aluminum removal percentage in port P_1.

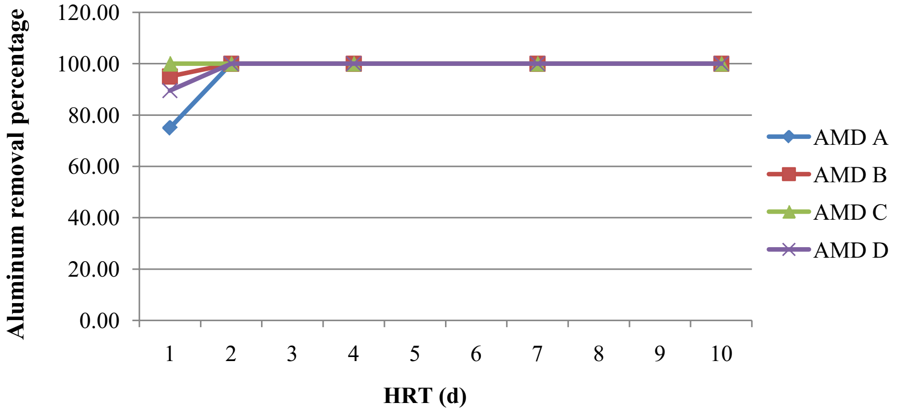

Fig. 13. Aluminum removal percentage in port P_2.

Williams [22]. It has been seen that manganese is the most difficult metal to remove from AMD because its solubility product is very high as compared to iron and aluminum. Manganese starts removing when the pH of the AMD solution reaches near 8.00 and above.

3.8. Sulfate removal behavior in SAPS

The cumulative removal of sulfate is observed to amplify with higher retention time. For 1 d HRT, it has been observed that a minimum cumulative removal of sulfate was 455 mg/L at the discharge of the SAPS unit (port P_3).

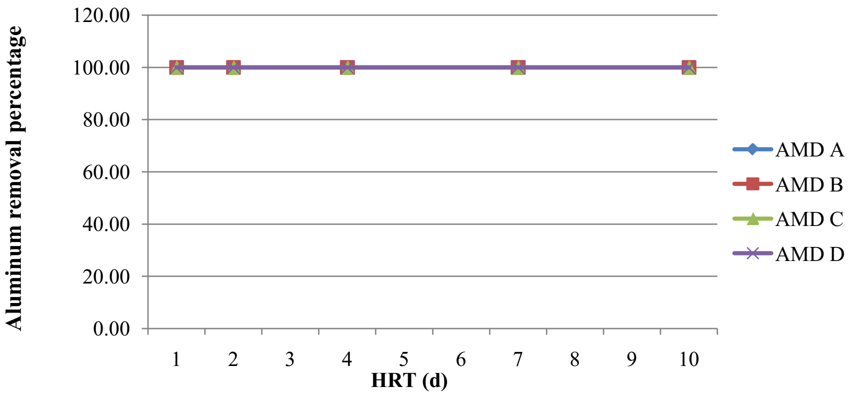

Fig. 14. Aluminum removal percentage in port P_3.

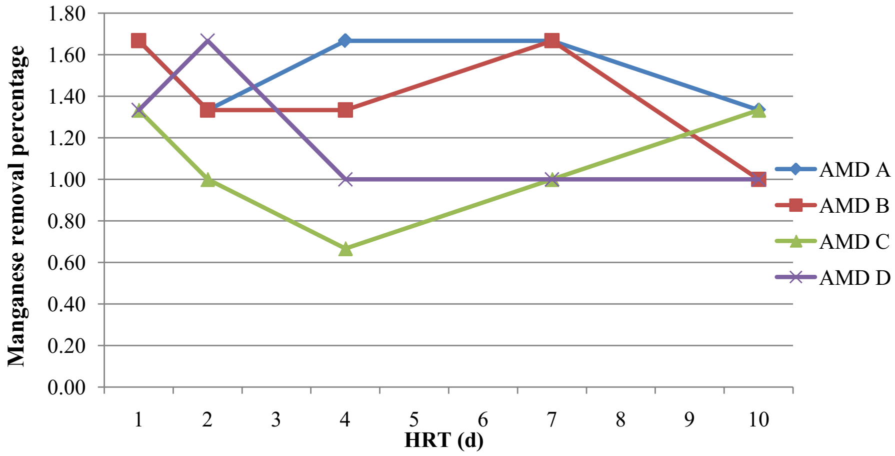

Fig. 15. Manganese removal percentage in port P_1.

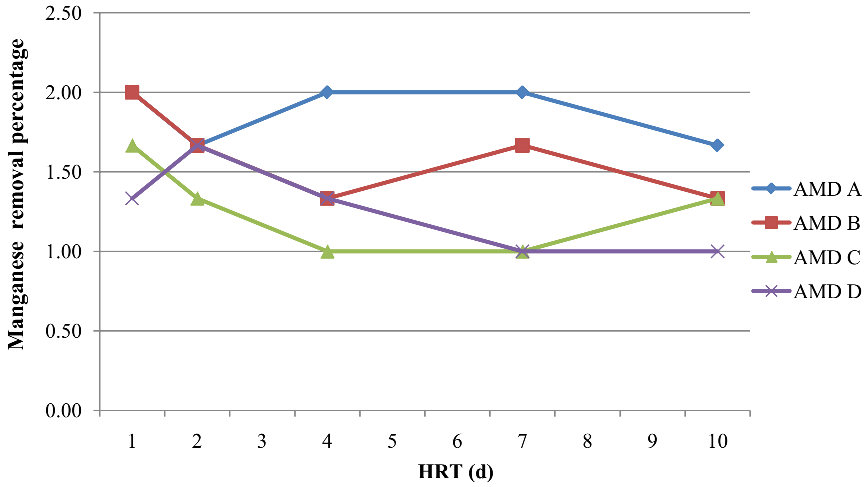

Fig. 16. Manganese removal percentage in port P_2.

For AMD A, it has been observed that maximum cumulative removal of sulfate, that is, 534 mg/L occurred in 10 d HRT at port P_3 for HRT of 10 d, for AMD A. Hence, during the SAPS process the sulfate concentration was observed to be decreasing from influent inlet to its discharge. Similar trends of sulfate removal were observed for the other three AMDs, that is, AMD B, AMD C, and AMD D. The results of sulfate removal are presented in Table 3.

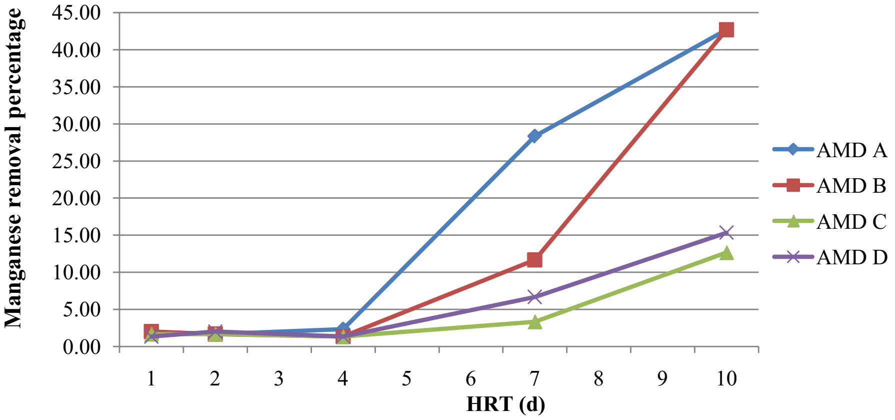

Fig. 17. Manganese removal percentage in port P_3.

Table 3
Results of sulfate removal for different HRTs at port P_3 (mg/L)

AMD	Initial sulfate concentration	HRT				
		1 d	2 d	4 d	7 d	10 d
AMD A	1,031	455	490	510	520	534
AMD B	1,037	458	493	511	523	538
AMD C	1,041	460	495	514	525	538
AMD D	1,036	460	495	511	524	540

4. Conclusions

The effectiveness of the laboratory SAPS for AMD treatment was investigated in this study. The effect of ferric/ferrous ratio along with total iron (iron factor, *F*) of influent AMD and HRT on alkalinity generation was studied. In addition to the above, iron, aluminum, and manganese removal behavior were also studied in detail. Based on the experimental studies, some key findings have been obtained as follows:

- It is observed that the alkalinity generation is increasing with an increase in the iron factor, ($F = R \times TI$) for a particular HRT at constant aluminum and manganese concentration in influent AMDs.
- The increase in alkalinity generation is higher for longer HRT for a particular iron factor ($F = R \times TI$) at constant aluminum and manganese concentration in influent AMDs.
- It was evident that the alkalinity generation by SAPS increases in a logarithmic manner with an increase in HRT for a particular AMD.
- Experimental breakthrough curves of removal of iron and aluminum demonstrated that there was 100% removal of iron and aluminum were observed in SAPS treatment for 7 d HRT. Hence SAPS proved to be much effective in the treatment of high iron and aluminum-containing AMD.
- The maximum manganese removal up to 42.67% for AMD A was observed because a much higher pH level (8–10) is required for complete removal of manganese.
- The sulfate reduction took place gradually in SAPS which indicated that the sulfate was being consumed by sulfate-reducing bacteria, as a result metals were being removed and alkalinity generated.
- This work provides an approach for the effective and efficient design of SAPS for the treatment of AMDs.

Acknowledgment

The author would like to express their sincere gratitude to the Department of Mining Engineering, NIT, Raipur, for their help, support and their kind co-operation during this study.

References

[1] I. Moodley, C.M. Sheridan, U. Kappelmeyer, A. Akcil, Environmentally sustainable acid mine drainage remediation: research developments with a focus on waste/by-products, Miner. Eng., 126 (2018) 207–220.
[2] D.B. Johnson, Chemical and microbiological characteristics of mineral spoils and drainage waters at abandoned coal and metal mines, Water Air Soil Pollut., 3 (2003) 47–66.
[3] A. Akcil, S. Koldas, Acid mine drainage (AMD): causes, treatment and case studies, J. Cleaner Prod., 14 (2006) 1139–1145.
[4] R.A. Koski, L. Munk, A.L. Foster, W.C. Shanks III, L.L. Stillings, Sulfide oxidation and distribution of metals near abandoned copper mines in coastal environments, Prince William Sound, Alaska, USA, Appl. Geochem., 23 (2008) 227–254.
[5] R.S. Hedin, G.R. Watzlaf, R.W. Nairn, Passive treatment of acid mine drainage with limestone, J. Environ. Qual., 3 (1994) 1338–1345.
[6] G.R. Watzlaf, K.L. Schroeder, R.L.P. Kleinmann, C.L. Kairies, R.W. Nairn, The Passive Treatment of Coal Mine Drainage, DOE/NETL-2004/1202, 2004, p. 72.
[7] J.A. Jacobs, J.H. Lehr, S.M. Testa, Acid Mine Drainage, Rock Drainage, and Acid Sulfate Soils: Causes, Assessment, Prediction, Prevention, and Remediation, John Wiley & Sons, Inc., Somerset US, 2014, p. 520.
[8] C. Zipper, J. Skousen, C. Jage, Passive Treatment of Acid-Mine Drainage, Powell River Project, Publication, 460–133 (2011) 1–6.
[9] C.A. Cravotta III, C.S. Kirby, Acidity and Alkalinity in Mine Drainage: Practical Considerations, Proceedings American Society of Mining and Reclamation, 2004, pp. 334–365.
[10] N. Kuyucak, Acid Mine Drainage Prevention and Control Options, Mine Water & Environment, IMWA Congress Sevilla, Spain, 2012, pp. 599–606.

[11] C.R. Jage, Water Quality Based Design Guidelines for Successive Alkalinity-Producing System Used in the Treatment of Acidic Mine Drainage, M.S. Thesis Virginia Polytechnic Institute and State University, Blacksburg Virginia, 2000, p. 80.

[12] H.L. Yadav, A. Jamal, Treatment of acid mine drainage: a general review, Int. Adv. Res. J. Sci., Eng. Technol., 3 (2016) 116–122.

[13] D.A. Kepler, E.C. McCleary, Successive Alkalinity-Producing Systems (SAPS) for the Treatment of Acidic Mine Drainage, Proceeding America Society of Mining and Reclamation, 1994, pp. 195–204.

[14] M.D. Patel, R.K. Jade, P.K. Dewangan, Study of performance of laboratory successive alkalinity producing system (SAPS) with reference to metal removal and alkalinity generation during acid mine drainage treatment, Res. J. Chem. Environ., 28 (2019) 2278–4527.

[15] R.B. Baird, A.D. Eaton, E.W. Rice, Standard Methods for the Examination of Water and Wastewater, APHA-AWWA-WEF, Washington, D.C., 23rd ed., 2017.

[16] R.P. Choudhary, A.S. Sheoran, Performance of single substrate in sulphate reducing bioreactor for the treatment of acid mine drainage, Miner. Eng., 39 (2012) 29–35.

[17] R.P. Choudhary, A.S. Sheoran, Comparative study of cellulose waste versus organic waste as substrate in a sulfate reducing bioreactor, Bioresour. Technol., 102 (2011) 4319–4324.

[18] T. Genty, B. Bussière, M. Benzaazoua, C.M. Neculita, G.J. Zagury, Changes in efficiency and hydraulic parameters during the passive treatment of ferriferous acid mine drainage in biochemical reactors, Mine Water Environ., 37 (2018) 686–695.

[19] G.J. Yim, S.W. Ji, Y.W. Cheong, C.M. Neculita, H. Song, The influences of the amount of organic substrate on the performance of pilot-scale passive bioreactors for acid mine drainage treatment, Environ. Earth Sci., 73 (2015) 4717–4727.

[20] A. Ordonez, J. Loredo, F. Pendas, A Successive Alkalinity Producing System (SAPS) as Operational Unit in a Hybrid Passive Treatment System for Acid Mine Drainage, Mine Water and Environ, IMWA Congress, Sevilla, Spain, 1999, pp. 9–35.

[21] K.B. Hallberg, D.B. Johnson, Biological manganese removal from acid mine drainage in constructed wetlands and prototype bioreactors, Sci. Total Environ., 338 (2005) 115–124.

[22] D.J. Sapsford, K.P. Williams, Sizing criteria for a low foot print passive mine water treatment system, Water Res., 43 (2009) 423–432.